Identification of Structural Parameters Based on PZT Impedance Using Genetic Algorithms

Y. H. Hu, Y. W. Yang, L. Zhang and Y. Lu

Abstract—**Electromechanical (EM) impedance method for structural health monitoring (SHM) is based on detecting the changes of the measured signatures of the Lead Zirconate Titanate (PZT) EM admittance (the inverse of the impedance). Although this method has been successfully applied for various engineering structures for damage detection, it is unable to specify the effect of damage on structural properties. The direct indicator of the structural properties is the structural mechanical impedance which can be extracted from the PZT EM admittance signatures. To model the structural impedance, this paper presents a multiple-degrees-of-freedom system consisting of a number of one-degree-of-freedom elements with mass, spring and damper components. Genetic algorithms (GAs) are employed to search for the optimal solution of the unknown dynamic system parameters by minimizing an objective function. Experiment has been carried on a two-storey concrete frame subjected to base vibrations that simulate earthquake. A number of PZT transducers are regularly arrayed and bonded to the frame structure to acquire PZT EM admittance signatures. The changes of the structural parameters in the model system are quantified using GAs. The relation between the distance of the PZT transducer away from the damage and the changes of the structural parameters identified by the PZT transducer is studied. Finally, the sensitivity of the PZT transducers is discussed.**

I. Introduction

Many civil engineering structures after suffering a natural disaster, such as an earthquake, can be still in service. However, the strength and the serviceability of these structures are questionable due to the possible damage induced in the structures. Even a minor incipient damage carries the potential to lead to a catastrophic impact on lives and properties. Because of this effect, the development of real-time, in-situ structural health monitoring (SHM) and damage detection techniques has been stimulated. In virtue of Lead Zirconate Titanate (PZT) transducers, the electromechanical (EM) impedance method has been developed to be a powerful way to detect structural damage. This method detects the changes of EM admittance (the inverse of the impedance) signatures of the PZT transducer which is surface bonded to the host structure. The first model of the PZT driven structural dynamic system was proposed in [1] and subsequently applied in various engineering structures [2]-[6]. However, the EM impedance method can only be used to predict the existence of the structural damage but not to further investigate the influence of the damage on the structural properties. It is the structural mechanical impedance that reflects the effects of the structural dynamic properties directly. The structural mechanical impedance can be extracted from the raw EM admittance signatures by means of signature decompositions [7]. A structural impedance model is expected to quantitatively relate the damage state to the changes of structural properties. Towards this goal, a multiple–degrees-of-freedom (MDOF) system model is proposed, which is composed of a number of single-degree-of-freedom (SDOF) elements with mass, spring and damper components. The unknown parameters of mass, stiffness and damping coefficients in each SDOF element can be derived by fitting the structural impedance of the model system with that extracted from the raw experimental data of the PZT EM admittance signatures.

Evolutionary computation (EC) based on the heuristic concepts of natural selection have developed into a group of powerful techniques for search and optimization, involving evolutionary programming (EP), evolutionary strategies (ES), genetic programming (GP), and genetic algorithms (GAs). Among them, the GAs is used in this study. The concept of GAs was firstly introduced in [8] and has been successfully applied in various engineering areas [9]. The well known applications include scheduling and sequencing, vehicle routing and scheduling, group technology, facility layout and location, transportation, structural optimization, and inverse problem solving [10]-[16]. GAs have also been employed for structural damage detection. For instance, GAs were used to locate and identify structural damage from measured natural frequencies and mode shapes [17]. In [18], genetic and eigensensitivity algorithms were used to optimize the discrete damage location variables and the damage severity, respectively. As a method of detecting the location of structural damage, a GA was used to optimize the fitness functions formulated in terms of static measured displacements [19]. In [20] an improved GA and a local optimizer were applied for flaw detection of composites from scattered elastic-wave field. To identify the structural damage, a GA with real number encoding was applied to minimize the objective function, which directly compares the changes in the measurements before and after damage [21]. And recently, an approach for detecting damage based on a

Y. H. Hu is with the School of Civil and Environmental Engineering, Nanyang Technological University, 50 Nanyang Avenue, Singapore (e-mail: huyu0006@ntu.edu.sg).

Y. W. Yang is with the School of Civil and Environmental Engineering, Nanyang Technological University, 50 Nanyang Avenue, Singapore (e-mail: cywyang@ntu.edu.sg).

L. Zhang is with the School of Civil and Environmental Engineering, Nanyang Technological University, 50 Nanyang Avenue, Singapore (e-mail: lanezhang@pmail.ntu.edu.sg).

Y. Lu is with the Institute for Infrastructure and Environment, School of Engineering and Electronics, University of Edinburgh, Edinburgh, EH9 3JL, UK (e-mail: Yong.Lu@ed.ac.uk)

1-4244-1340-0/07/$25.00 ©2007 IEEE

continuum damage model using a GA was presented [22].

In this paper, the GAs are used to search for the optimal values of structural parameters in the structural impedance model by minimizing a specified fitness function. The fitness evaluation function is defined as the root mean square deviation between the structural impedance values from the theoretical model and those derived from the experimentally measured PZT EM admittance. The optimal values of structural parameters derived before and after the appearance of structural damage are compared to quantitatively analyze the changes of structural properties associated with the damage state. The PZT transducers regularly bonded to a concrete frame are of different distances from the damage. Therefore, a reasonable relation between the changes of structural parameters and the distance of the PZT transducer from the damage can be established and the sensitivity of the PZT transducer to structural damage is discussed.

II. Electro-Mechanical Impedance Technique

A. PZT EM Admittance

The first EM impedance model of the PZT-structure interaction system was proposed in [1], in which the host structure was simplified as a skeletal structural and the PZT transducer as a thin bar undergoing axial vibration. Based on the piezoelectric effect of imparting mechanical strain when subjected to an electric field and the converse piezoelectric effect of generating electric charges in response to a mechanical strain, the EM admittance of the PZT transducer was expressed as

$$Y(\omega) = j\omega \frac{w_a l_a}{h_a}\left(\left(\bar{\varepsilon}_{33}^{T} - d_{31}^{2}\bar{Y}^{E}\right) + \left(\frac{Z(\omega)}{Z(\omega)+Z_a(\omega)}\right) d_{31}^{2}\bar{Y}^{E}\left(\frac{\tan \kappa l_a}{\kappa l_a}\right)\right) \quad (1)$$

where Z_a and Z are the mechanical impedances of the PZT and the host structure, respectively; j is the imaginary unit; ω is the angular frequency of the driving voltage; w_a, l_a and h_a are the width, length and thickness of the PZT transducer, respectively; $\bar{Y}^{E} = Y^{E}(1+j\eta)$ is the complex Young's modulus of the PZT material at zero electric field; d_{31} is the piezoelectric constant; $\bar{\varepsilon}_{33}^{T} = \varepsilon_{33}^{T}(1-j\delta)$ is the complex dielectric constant; η and δ denote the mechanical loss factor and the dielectric loss factor of the PZT material, respectively; κ is the wave number which is related to the angular frequency of excitation ω by $\kappa = \omega\sqrt{\rho/\bar{Y}^{E}}$; and ρ is the material density of the structure.

Equation (1) indicates that the EM admittance of PZT transducer is directly related to the mechanical impedance of the host structure. Therefore, any change in the EM admittance signatures is the indication of a change in the structural integrity which may be caused by the appearance of structural damage.

B. Extraction of Structural Mechanical Impedance

In form of Cartesian coordinates, the complex mechanical impedance of the host structure and the PZT transducer are expressed as

$$Z = x + jy \quad (2)$$

$$Z_a = x_a + jy_a \quad (3)$$

where x, y and x_a, y_a are the real and imaginary parts of the structural mechanical impedance and the PZT mechanical impedance, respectively.

Substituting (2) and (3) into (1) and solving the complex equation (1), we can obtain

$$x = \frac{-K\omega\left(c(r-\eta t)+(t+\eta r)\right)\left(y_a D + x_a\right)}{G_A\left(1+D^2\right)} - x_a \quad (4)$$

$$y = D\left(x + x_a\right) - y_a \quad (5)$$

where

$$K = \frac{w_a l_a}{h_a} d_{31}^{2} Y^{E} \quad (6)$$

$$c = \frac{\left(G_A / B_A\right)(r-\eta t)+(t+\eta r)}{\left(G_A / B_A\right)(t+\eta r)-(r-\eta t)} \quad (7)$$

$$D = \frac{y_a - c x_a}{c y_a + x_a} \quad (8)$$

where r and t can be obtained from the following equation

$$r + jt = \frac{\tan \kappa l_a}{\kappa l_a} \quad (9)$$

and G_A and B_A can be obtained from

$$G_A + jB_A = Y - j\omega \frac{w_a l_a}{h_a}\left(\bar{\varepsilon}_{33}^{T} - d_{31}^{2}\bar{Y}^{E}\right) \quad (10)$$

Following this computational procedure, the structural impedance can be extracted from the measured admittance signature of the PZT transducer. In this computation, r and t must be determined precisely from (9) using the complex algebra [23].

III. Modeling of Structural Impedance

The concept of structural mechanical impedance is analogous to the electrical impedance. Structural mechanical impedance at a given point can be defined as the ratio of a sinusoidal force applied to the system at that point to the velocity at the same point [24]. For an SDOF mass-spring-damper element subjected to an excitation force shown in Figure 1, the mechanical impedance of the structure is [23]

$$|Z| = \frac{F_o}{\dot{x}_o} = \sqrt{c^2 + \left(\frac{m\omega^2 - k}{\omega}\right)^2} \quad (11)$$

where the subscript '*o*' denotes the amplitudes of the variables. Using complex notation, analogous to that used in classical electricity, the structural mechanical impedance, *Z*, can be expressed as

$$Z = x + yj = c + \left(\frac{m\omega^2 - k}{\omega} \right) j \tag{12}$$

Equation (12) is meant for an SDOF system. For a complex structural system, the impedance model discussed above can be easily extended to be an MDOF system by combining a number of SDOF elements.

For a parallel connection system, the combined mechanical impedance, Z_p can be expressed as the sum of the impedances, Z_i of each element.

$$Z_p = \sum_{i=1}^{n} Z_i \tag{13}$$

For a series connection system, the combined mechanical impedances, Z_s can be expressed as

$$\frac{1}{Z_s} = \sum_{i=1}^{n} \frac{1}{Z_i} \tag{14}$$

IV. Overview of Genetic Algorithm

A. General Structure of GAs

The original GA was developed based on the Darwinian theory of natural evolution [8]. Later on, the more practical form of GAs was described in [9]. Differing from the conventional search techniques, GAs are stochastic search techniques starting with an initial population of randomly generated candidate solutions encoded as chromosomes. The chromosomes evolve through successive generations. During each generation, offspring are created from the parents by means of crossover and mutation. A new generation is formed by selecting chromosomes according to their level of fitness in the problem domain. Fitter chromosomes have higher possibilities of being selected. After a number of generations, the algorithms converge to the best chromosome which hopefully represents the optimal solution to the problem.

B. Operators of GAs

To obtain better-fit chromosomes, three basic genetic operators (i.e., selection, crossover and mutation) are involved in GAs. Selection is a process in which a mating pool of individual chromosomes of the current generation is chosen in a certain way for reproduction of the next generation according to the fitness value. In this paper, the selection algorithm known as "roulette wheel" selection has been used, with which the probability of selection is proportional to the fitness of the chromosome. Crossover is a main genetic operator, which operates on two randomly selected chromosomes at a time and generates offspring by exchanging part of the parents' genes. In the one-point crossover scheme, the crossover rate is defined as the ratio of the number of offspring produced in each generation to the population size, which is used to regulate the solution space. Mutation is a background operator which produces spontaneous random changes in one or more chromosomes' genes. In GAs, this operator serves to introduce new materials in the population.

C. Objective Function

The GAs attempt to find the best solution to a given problem by minimizing an objective evaluation function which is called fitness function. In order to formulate the structural parameter identification problem into an optimization problem for the GAs to solve, it is necessary to specify an objective function which is used to provide a measure of how individuals have performed in the problem domain. The fittest individuals will have the lowest numerical value of the associated objective function.

Structural damage, especially local damage, is typically related to changes in the structural physical parameters. Therefore, to recognize the changes of structural parameters is a direct way to predict structural damage and also an effective way to assess the severity of the damage. Towards this goal, a model of driven point structural impedance with pending structural parameters should be set up. In this study, the proposed model is an MDOF system constructed by the connection of a number of SDOF elements as described in the former section. In this model, the structural impedance is a function of excitation frequency with unknown structural parameters, i.e., the mass m_i, the stiffness k_i and the damping coefficient c_i of each SDOF element. On the other hand, by means of decomposition we can obtain the signature of structural impedance from the experimentally measured PZT EM admittance. For an effective impedance model, the modeled structural impedance and the measured structural impedance should be approximately of the same value under the same excitation frequency. Since the real part of the structural mechanical impedance is more sensitive to the structural damages [25], the objective function for identifying structural parameters is defined as

$$f(m_1, k_1, c_1, m_2, k_2, c_2, \cdots, c_n) = \sqrt{\frac{\sum_{i=1}^{p} \left(x_i^e - x_i^t \right)^2}{\sum_{i=1}^{p} \left(x_i^e \right)^2}} \tag{15}$$

where, m_i, k_i and c_i ($i=1 \cdots n$) are the unknown mass, stiffness and damping coefficients of each SDOF element used to construct the MDOF model; n is the total number of the SDOF elements in the model; x_i and y_i ($i=1 \cdots p$) are the real and imaginary parts of the structural mechanical impedance under the excitation frequency of the *ith* sample point; p is the total number of sample points; and the superscripts 'e' and 't' denote the experimental data and theoretical data of the

corresponding variables respectively. The GAs are applied to search for the optimal values of the unknown structural parameters in the MDOF model system such that the fitness function in (15) is minimal.

D. Damage Assessment

Using the GAs, the optimal values of structural parameters in the model of the PZT driven point structural impedance can be derived according to the measured EM admittance signatures. For damage assessment, these optimal values obtained before and after the appearance of structural damage are compared to study the effects of damage on the structural properties, which are specified to be mass, stiffness and damping in this study. To quantify the effects of damage, the summation of the deviation of a certain parameter in each element is expressed as

$$\Delta_m = \sum_{i=1}^{n} \left(m_i^a - m_i^b \right) \tag{16}$$

$$\Delta_k = \sum_{i=1}^{n} \left(k_i^a - k_i^b \right) \tag{17}$$

$$\Delta_c = \sum_{i=1}^{n} \left(c_i^a - c_i^b \right) \tag{18}$$

where Δ_m, Δ_k and Δ_c are the sum of the deviation of mass, stiffness and damping coefficients in each SDOF element respectively; and the superscripts '*b*' and '*a*' denote the values at the health state and the damage state respectively.

V. Application for Detecting Seismic Induced Damage

A. Experimental Set-up and Procedure

In this study, an experiment was carried out on a two-storey concrete frame instrumented with five PZT transducers, as shown in Figure 2, where the dimensions and sizes of various structural members, i.e., the beams and columns, are indicated. The five PZT transducers were regularly bonded to one of the columns on the first floor of the frame structure. The suitable locations of the PZT transducers were determined based on the structural analysis and the engineering experience that cracks most probably appear at the joint section between the columns and beams. Therefore, the PZT transducers were bonded close to a joint and along a column in order to capture the information of vital structural damages. The dimensions and material properties of the PZT transducers are listed in Table I and their locations are listed in the second column of Table II. The concrete frame structure is placed on a shake table which generates base vibrations to simulate the earthquake. The concrete frame and the equipments used in this experiment are shown in Figure 3. The five PZT transducers were individually connected to different channels of a switch box, which was used to make a multiple connections between the HP 4192A Impedance Analyzer and the PZT transducers. The Impedance Analyzer excited the PZT transducers and simultaneously recorded the admittance signatures received by the PZT transducers. A sinusoidal sweep voltage with amplitude of 1 volt is applied to the PZT transducers over various frequency ranges. The Impedance Analyzer was then connected to a personal computer to store the data. In order to facilitate the automation of testing, the program VEE Pro v.6.01 was used to control the Impedance Analyzer via a GPIB interface card installed in the computer.

The test loads were applied in the form of the horizontal base motions with different frequencies. The test was performed in several phases and the sequences of the applied base motions are listed in Table III. The concrete frame structure was subjected to two main vibration phases, namely phase 2 and phase 4 as listed in Table III. The other three random vibration phases were used for structural identification. After vibration phase 2, incipient damages occurred in the structure, and some are visible. After vibration phase 4, major cracks appeared in the structure, especially at the joint section. The appearance of cracks on the column where the PZT transducers were installed is shown in Figure 4. The five PZT transducers were scanned before the base-loading in order to record the baseline signatures for the health condition. Under the conditions of incipient damage as shown in Figure 4(b) and serious damage as shown in Figure 4(c), the PZT transducers were individually scanned to acquire the post-damage signatures. The distances of the five PZT transducers from the main crack shown in Figure 4(c) are listed in the third column of Table II.

B. Results and Discussion

1) Application of GAs: All the EM admittance signatures captured by the five PZT transducers were used to derive the optimal values of the structural parameters of the MDOF model system. In this study, by means of trial and error the model of a parallel connection of a number of SDOF mass-spring-damper elements was used to successfully fit the signatures of structural impedance extracted from the measured PZT EM admittance. The main idea for the optimization problem in this study is to minimize the differences between the modeled structural impedances and the experimentally measured ones by searching the proper values for the structural parameters using the GAs.

The number of SDOF elements used to construct the structural impedance model is 32. Correspondingly, the total number of the unknown structural parameters in this model is 96, with the consequence as m_1, k_1, c_1, m_2, k_2, c_2,$\cdots\cdots m_{32}$, k_{32}, c_{32}. Each parameter is coded into 20-bit binary number and then the 96 parameters are translated into a chromosome of 1920 bits length. A GA with single-point crossover is employed with the probability of crossover of 0.8, probability of mutation of 0.01 and the population size of 20.

The structural impedance is meant for the PZT driven point, therefore it varies at different locations where the PZT transducer are bonded. Figure 5 shows the theoretically modeled and experimentally measured signatures of the structural impedance at the location where PZT patch 4 was

bonded for three structural states, i.e., no damage, incipient damage, and serious damage. The signatures for the locations where the other four PZT transducers were attached are very similar to Figure 5 and thus not shown for conciseness. From Figure 5 we can observe that for the three structural states, the theoretical and experimental results of the driven point structural impedance match very well. These results validate the proposed model for driven point structural impedance, which is composed of the series connection of 32 SDOF elements. It also validates the feasibility of GAs for acquiring the optimal solutions for structural parameters.

2) Convergence Performance: To evaluate the performance of the GAs for identification of structural parameters in the proposed structural impedance model, a study of the convergence of the fitness value should be performed. The convergence performances for the case of PZT patch 4 under three structural states are shown in Figure 6. In general, the convergence is stable and at the final stage of searching, the convergence of performance slows down significantly, which is typical for the GAs. Therefore, for all these three cases, the performance of the GAs in searching the optimal values of the structural parameters is satisfactory.

3) Sensitivity to Damage Detection: In order to relate the damage states to the quantitative changes of the structural properties, the optimal values of the structural parameters in the model are derived by the GAs, and the changes of each structural parameter are calculated as described in (16)-(18). Under the two structural damage states in this experiment, the changes of each structural parameter are calculated and illustrated in Figures 7, 8 and 9.

Figure 7 shows the changes of damping coefficient in the driven-point structural impedance model under two damage states. As all the values of the changes are positive, it can be concluded that the damping of the PZT driven points increases after the appearance of the structural damages. And at the same distance of PZT transducer from the damage, the absolute changes of damping are relatively larger for damage phase 2 than those for damage phase 1. It can be concluded that the more severe the damage, the more changes of the damping will be. From this figure, we can also observe that the larger the distance, the smaller the absolute value of the change is. This result indicates that the PZT transducer with larger distance from the damage is of lower sensitivity to the damage.

Figure 8 shows the changes of stiffness in the driven-point structural impedance model under the two damage states. As all the values of the changes are negative, it means that the stiffness of the driven points decreases after the appearance of the structural damages. And for the same distance of PZT transducer from the damage, the absolute changes of stiffness for damage phase 2 are mostly larger than those for damage phase 1. Similarly, it can be concluded that a severer damage will render more changes in stiffness, which is much easier to be detected by the PZT transducer. This figure again confirms that the PZT transducer with larger distance from the damage is less sensitive to the damage.

Figure 9 shows the changes of mass in the driven-point structural impedance model under the two damage states. For damage phase 1, the changes of mass exhibit no regularity, and vary around zero line. This indicates that the incipient damage has very limited effect on the mass. For damage phase 2, the changes are all negative, which shows that the severe damage leads to the reduction of the driven point mass. Since the absolute values of changes decrease as the distance of the PZT transducer from the damage increases, we can conclude again that the sensitivity of the PZT transducer to structural damage decreases as the distance increases.

VI. CONCLUSION

A model of the PZT driven point structural impedance for quantitative detection of the influence of the damage on the structural properties using the GAs has been presented. The structural parameters in the model are derived by minimizing an objective function based on the experimentally measured data of PZT EM admittance. Optimal values for each structural parameter derived before and after the appearance of structural damages are compared to analyze the changes of structural properties caused by the damage. An experiment has been carried out on a two-storey concrete frame subjected to base vibration which simulates the earthquake. Five PZT transducers have been regularly bonded to one of the column of the frame structure and scanned to acquire the signatures of the PZT EM admittance before and after the damage. For this case, the model of a series connection of 32 SDOF mass-spring-damper elements has been successfully used to fit the experimentally measured data. It is worth mentioning that the structural impedance model may be composed of the SDOF elements by different ways of connection, depending on the material of the structure and the excitation frequency. Using the GAs, the changes of the structural parameters caused by the structural damage in the model have been derived and analyzed. The results have demonstrated that the appearance of damage leads to increase in damping and decrease in stiffness and mass at the driven point, and that the model is more sensitive to the severe damage. It has also been concluded that the PZT transducer with larger distance from the damage is less sensitive to the damage. And this conclusion coincides with the previous studies of PZT sensing region based on the damage index techniques [25, 26]. In the end, it should be mentioned that the results derived from using GAs are just for one run. Several runs have been conducted and similar results have been obtained. The consistency of the results from different runs should be studied in the future research work.

REFERENCES

[1] C. Liang, F. P. Sun, and C. A. Rogers, "Coupled electromechanical analysis of adaptive material systems-determination of the actuator power consumption and system energy transfer," *Journal of Intelligent Material Systems and Structures*, vol. 5, pp. 12-20, 1994.

[2] J. W. Ayres, F. Lalande, Z. Chaudhry, and C. A. Rogers, "Qualitative impedance-based health monitoring of civil infrastructures", *Smart Materials and Structures*, vol. 7, no. 5, pp. 599-605, 1998.

[3] G. Park, K. Kabeya, H. H. Cudney, and D. J. Inman, "Impedance-based structural health monitoring of civil structural components," *ASCE Journal of Infrastructure Systems*, vol. 6, no. 4, pp. 153-160, 2000.

[4] G. Park, H. H. Cudney, and D. J. Inman, "Feasibility of using impedance-based damage assessment for pipeline structures," *Earthquake Engineering and Structural Dynamics*, vol. 30, pp. 1463-1497, 2001.
[5] V. Giurgiutiu, A. N. Zagrai, and J. J. Bao, "Piezoelectric wafer embedded active sensors for aging aircraft structural healthy monitoring," *International Journal of Structural health monitoring*, vol. 1, pp. 41-61, 2002.
[6] Y. W. Yang, J. F. Xu, and C. K. Soh, "Generic impedance-based model for structure-piezoceramic interacting system." *J of Aerospace Engineering*, vol. 18, no. 2, pp. 93-101, 2005.
[7] S. Bhalla, and C. K. Soh, "Structural impedance based damage diagnosis by piezo-transducers", *Earthquake Engineering and Structural Dynamics*, vol. 32, no. 12, pp. 1897-1916, 2003.
[8] J. Holland, *Adaptation in Natural and Artificial Systems*, The University of Michigan Press, Ann Arbor, MI, 1975.
[9] D. Goldberg, *Genetic Algorithms in Search, Optimization and Machine Learning*, Addison-Wesley, New York, 1989.
[10] J. Blanton, and R. Wainwright, "Multiple vehicles routing with time and capability constraints using genetic algorithm," in *Proceedings of the 5th International Conference on Genetic Algorithms,* S. Forrest, (editor), Morgan Kaufmann Publishers, San Mateo, CA, 1993, pp. 452-459.
[11] J. Grefenstette, *Genetic Algorithm for Machine Learning*, Kluwer Academic Publishers, Norwell, MA, 1994.
[12] R. Cheng, and M. Gen, "Fuzzy vehicle routing and scheduling problem using genetic algorithms," in *Genetic Algorithms and Soft Computing*, F. Herrera, and J. Verdegay, (editors), Spring-Verlag, 1996, pp. 683-709.
[13] C. K. Soh, and J. P. Yang, "Fuzzy controlled genetic algorithm search for shape optimization," *Journal of Computing in Civil Engineering, ASCE*, vol. 10, no. 2, pp. 143-150, 1996.
[14] C. S. Krishnamoorthy, P. P. Venkatesh, and R. Sudarshan, "Object-oriented framework for genetic algorithms with application to space truss optimization," *Journal of Computing in Civil Engineering, ASCE*, vol. 16, no. 1, pp. 66-75, 2002.
[15] J. Li, and R. S. K. Kwan, " A fuzzy genetic algorithm for driver scheduling," *European Journal of Operational Research*, vol. 147, no. 2, pp. 334-344, 2003.
[16] E. M. R. Fairbairn, M. M. Silvoso, R. D. T. Filho, J. L. D. Alves, and N. F. F. Ebecken, "Optimization of mass concrete construction using genetic algorithm," *Computers & Structures*, vol. 82, pp. 281-299, 2004.
[17] C. Mares, and C. Surace, "An application of genetic algorithms to identify damage in elastic structures," *Journal of Sound and Vibration*, vol. 195, no. 2, pp. 195-215, Jan. 1996.
[18] M. I. Friswell, J. E. T. Penny, and S. D. Garvey, "A combined genetic and eigensensitivity algorithm for the location of damage in structures". *Computers & Structures*, vol. 69, pp. 547-556, Apr. 1998.
[19] J. Chou, and J. Ghaboussi, "Genetic algorithm in structural damage detection," *Computers & Structures*, vol. 79, pp. 1335-1353, Mar. 2001.
[20] Y. G. Xu, and G. R. Liu, "Detection of flaws in composites from scattered elastic-wave field using an improved μGA and a local optimizer," *Computer Methods in Applied Mechanics and Engineering*, vol. 191, pp. 3929-3946, Apr. 2002.
[21] H. Hao, and Y. Xia, "Vibration-based damage detection of structures by genetic algorithm," *Journal of Computing in Civil Engineering, ASCE,* vol. 16, no. 3, pp. 222-229, Jul. 2002.
[22] R. Perera, and R. Torres, "Structural damage detection via modal data with genetic algorithms," *Journal of Structural Engineering, ASCE*, vol. 132, no. 9, pp. 1491-1501, Sep. 2006.
[23] S. Bhalla, and C. K. Soh, "Structural impedance based damage diagnosis by piezo-transducers," *Earthquake Engineering and Structural Dynamics*, vol. 32, no. 12, pp. 1897-1916, 2003.
[24] E. L. Hixon, *Shock and Vibration Handbook*, 3rd ed., Mc Graw Hill Book Co., edited by C. M. Harris, New York, 1988, pp. 10.1-10.46.
[25] Y. H. Hu, and Y. W. Yang, "Sensing region of PZT transducers bonded to concrete," in *Proceedings of the 14th International Symposium on Smart Structures and Materials & Nondestructive Evaluation and Health Monitoring,* to be held in San Diego, California, USA, 18-23 March 2007.
[26] Y. H. Hu, and Y. W. Yang, "Wave propagation modeling of PZT sensing region for structural health monitoring." *Smart Materials and Structures*, (in press).

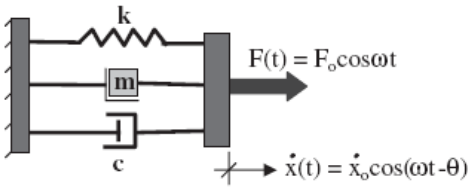

Fig. 1. A single degree of freedom system under dynamic excitation

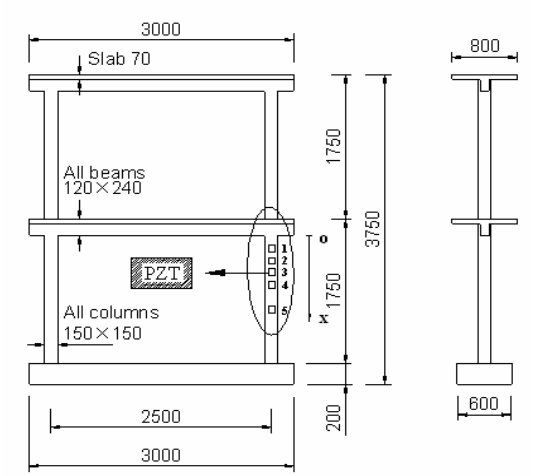

Fig. 2. Dimensions of concrete frame (Unit: mm)

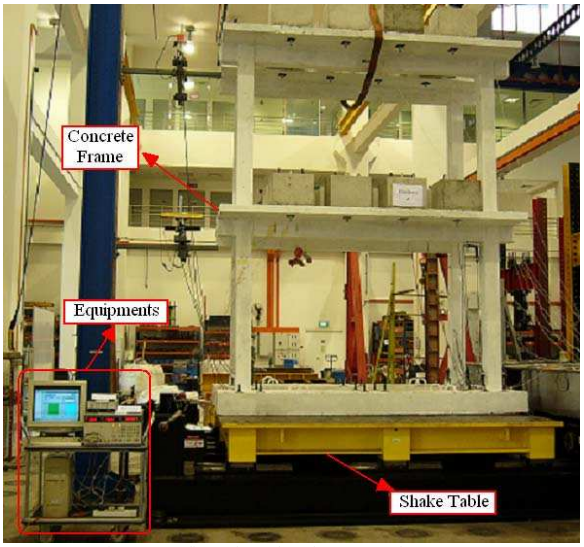

Fig. 3. Configuration of equipments and test structure

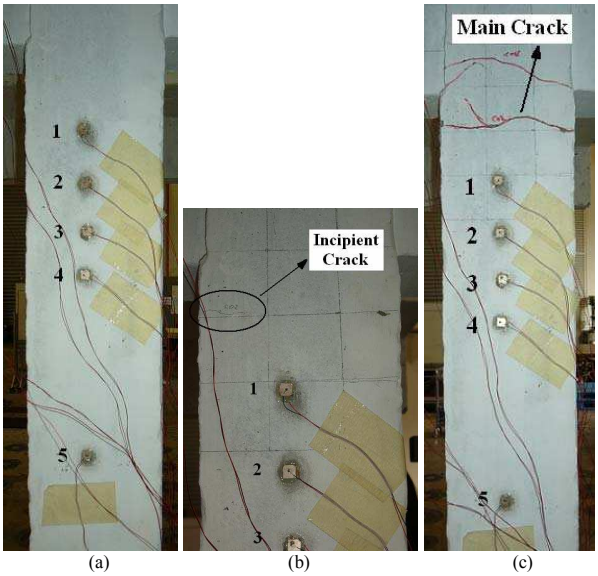

Fig. 4. Health states of the column: (a) health condition; (b) incipient damage condition; and (c) serious damage condition

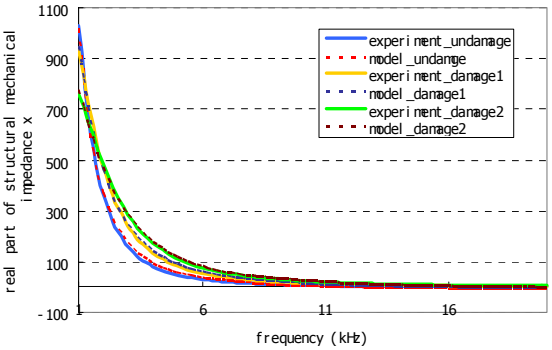

Fig. 5. Theoretical and experimental results of the real part of the PZT driven point structural impedance versus the distance of the PZT transducer from the damage under three structural states

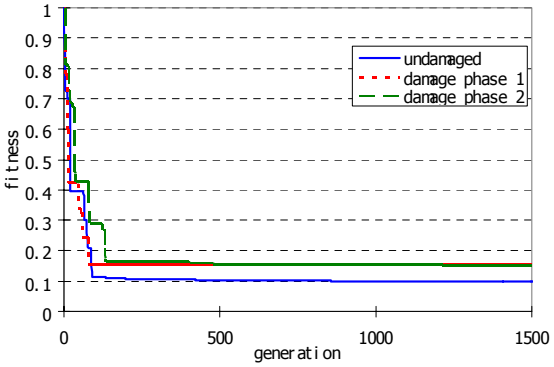

Fig. 6. Convergences of the GA applied to search for optimal solutions to structural parameters in the structural impedance model for the point driven by PZT patch 4 under three health conditions

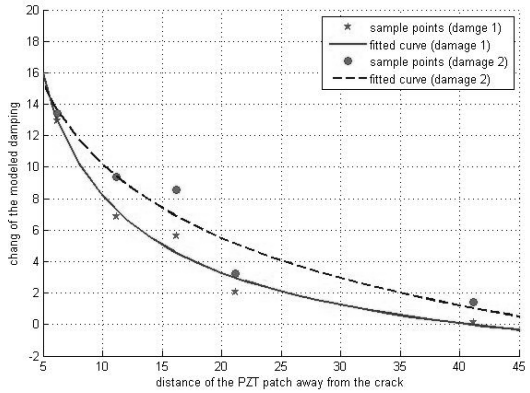

Fig. 7. Detected changes of damping in the impedance model for the driven points with different distances from the damage for two damage states

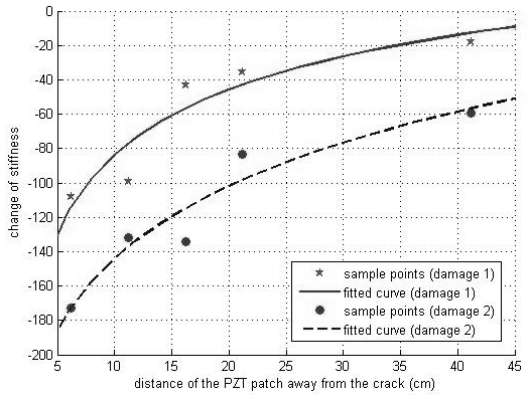

Fig. 8. Detected changes of stiffness in the impedance model for the driven points with different distances from the damage for two damage states

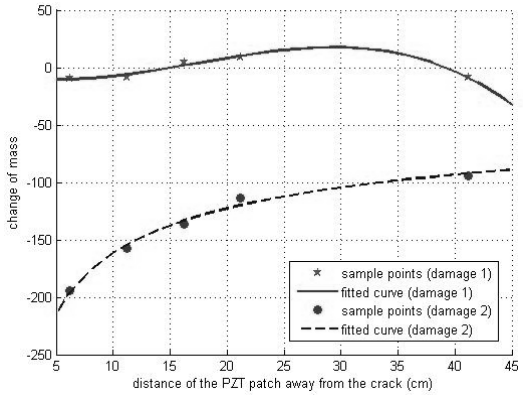

Fig. 9. Detected changes of mass in the impedance model for the driven points with different distances from the damage for two damage states

TABLE I
MATERIAL PROPERTIES AND DIMENSIONS OF PZT TRANSDUCERS

Symbol	Quantity	Practical Value
l_a	length	10 mm
w_a	width	10 mm
h_a	thickness	0.2 mm
Y	Young's modulus	66.7 GPa
η	loss factor	0.005
ρ	mass density	7800 kg/m^3
d_{31}	strain constant	-2.10E-10 m/volt
ε_{33}^T	permittivity	1.93E-08 fatad/m
δ	dielectric loss factor	1.50E-02

TABLE II
LOCATIONS OF PZT TRANSDUCERS AND THEIR DISTANCE FROM THE MAIN CRACK

Patch Number	Distance from the joint o along the column as shown in Figure 2	Distance of the PZT patch from the main crack
1	100 mm	62 mm
2	150 mm	112 mm
3	200 mm	162 mm
4	250 mm	212 mm
5	450 mm	412 mm

TABLE III
TEST SEQUENCE OF THE SHAKE TABLE

Phase Number	Name	Description	Purpose
1	RND-A	Random PGA=0.02g	Structural identification
2	CHL-023	Chile GPA=0.23g	Moderate shaking
3	RND-B	Random PGA=0.02g	Structural identification
4	CHL-046	Chile PGA=0.46g	Sever shaking
5	RND-C	Random PGA=0.02g	Structural identification